

The HELEEOS Atmospheric Effects Package: A Probabilistic Method for Evaluating Uncertainty in Low-Altitude, High-Energy Laser Effectiveness

**S. T. Fiorino,* R. J. Bartell, G. P. Perram, D. W. Bunch,
L. E. Gravley, C. A. Rice, Z. P. Manning, and M. J. Krizo**

*Center for Directed Energy, Air Force Institute of Technology, 2950 Hobson Way,
Wright-Patterson Air Force Base, Ohio 45433-7765*

and

J. R. Roadcap and G. Y. Jumper

*Battlespace Environment Division, Space Vehicles Directorate, Air Force Research
Laboratory, Hanscom Air Force Base, Massachusetts 01731-3010*

The Air Force Institute of Technology's (AFIT's) Center for Directed Energy, sponsored by the High Energy Laser Joint Technology Office (JTO), has developed the High Energy Laser End-to-End Operational Simulation (HELEEOS) parametric one-on-one-engagement-level model. HELEEOS incorporates scaling laws tied to respected wave optics codes and all significant degradation effects to include thermal blooming due to molecular and aerosol absorption, scattering extinction, and optical turbulence. The HELEEOS model enables the evaluation of uncertainty in low-altitude, high-energy laser (HEL) engagement due to all major clear-air atmospheric effects. Atmospheric parameters investigated include profiles of temperature, pressure, water vapor content, and optical turbulence as they relate to layer extinction coefficient magnitude. Worldwide seasonal, diurnal, and geographical spatial-temporal variability in these parameters is organized into probability density function (PDF) databases using a variety of recently available resources to include the Extreme and Percentile Environmental Reference Tables (ExPERT), the Master Database for Optical Turbulence Research in Support of the Airborne Laser, the Global Aerosol Data Set (GADS), and the Directed Energy Environmental Simulation Tool (DEEST) in conjunction with Air Force Weather Agency MM5 numerical weather forecasting data. Updated ExPERT mapping software allows the HELEEOS operator to choose from specific site or regional surface and upper air data to characterize correlated molecular absorption, aerosol absorption and scattering, and optical turbulence by percentile. The PDF nature of the HELEEOS atmospheric effects package enables realistic probabilistic outcome analyses that permit an estimation of the level of uncertainty in the calculated probability of kill (P_k).

Received November 30, 2004; revision received February 27, 2006.

*Corresponding author; e-mail: steven.fiorino@afit.edu.

HELEEOS users can additionally access, display, and export the atmospheric data independent of a HEL engagement simulation.

KEYWORDS: Aerosol extinction, Correlated atmosphere, HEL propagation, Percentile, Probabilistic

1. Introduction

The Air Force Institute of Technology's (AFIT's) Center for Directed Energy, sponsored by the High Energy Laser Joint Technology Office (JTO), has developed the High Energy Laser End-to-End Operational Simulation (HELEEOS) parametric one-on-one-engagement-level model. One of the primary purposes of the HELEEOS model is to provide realistic probabilistic outcome analyses that permit an estimation of the level of uncertainty in the calculated probability of kill (P_k) for lower tropospheric high-energy laser (HEL) engagements (such as is envisioned for the Air Tactical Laser). Despite its dependence on computationally fast scaling law codes, HELEEOS cannot fully incorporate all significant degradation effects into a P_k without a robust and probabilistic accounting of the simulated environment. This paper describes a method employed by HELEEOS to integrate correlated, probabilistic atmospheric effects, such as molecular absorption, aerosol extinction, and optical turbulence, into HEL effectiveness simulations. The paper further details how the above atmospheric effects are derived from basic meteorological and/or climatological parameters—or how those effects are directly predicted—for the simulation scenario selected. The HELEEOS model itself, its applied scaling laws, an overview of the interface, and a vision for its employment beyond the modeling and simulation community are addressed in Bartell et al.²

The HELEEOS approach to characterizing atmospheric effects is focused on assessing uncertainty in the ultimate P_k in clear-line-of-sight conditions. Even in such a “clear-sky” environment, the atmosphere significantly affects both beam spread and attenuation characteristics of HEL propagation. Thus, HELEEOS can produce useful analyses of HEL propagation uncertainty even with the restriction that there is a noncloudy path of propagation. However, assessing P_k uncertainty requires detailed knowledge of atmospheric uncertainty, which requires an expanded environmental database beyond the typical deterministic or “standard” atmospheric type data incorporated into many modeling scenarios.

The subsequent sections of this paper outline the environmental databases utilized by HELEEOS, data correlation techniques, the main contributors to HEL beam spread and attenuation, and preliminary findings. Under environmental databases, the Extreme and Percentile Environmental Reference Tables (EXPERT), the Global Aerosol Data Set (GADS), the Master Database for Optical Turbulence Research in Support of the Airborne Laser, and the Directed Energy Environmental Simulation Tool (DEEST) are described. The paper then presents details of the correlation technique and how it varies with altitude. How the effects of molecular absorption, aerosol scattering and absorption, and optical turbulence are incorporated is then addressed. Finally, a conclusion with proposals for future work and possible HELEEOS add-ons is offered.

2. Environmental Databases

The EXPERT database is a joint effort by the Air Force Research Laboratory's Air Vehicles and Space Vehicles Directorates and the Air Force Combat Climatology Center. EXPERT is an interactive microcomputer program to display precalculated climatological values for various regions—land, ocean, and upper air—as well as 289 sites worldwide. For the

individual surface land sites, this program allows the analyst to view monthly and hourly percentile data, duration data, and yearly minimum and maximum values for the following atmospheric variables: altimeter setting, dew point temperature, absolute humidity, relative humidity, specific humidity, temperature, wind speed, and wind speed with gusts. Percentiles for diurnal data and sky cover data are displayed as well. Also available are the percent frequency of occurrence for several “significant” weather phenomena: thunderstorms; fog, blowing snow or sand, freezing rain, hail, snow, and rain. Notably, ExpERT also enables the analyst to display the probabilities of when a particular combination of temperature and relative humidity will occur—for a specific land site.⁹

For the upper-air and ocean regions, where the climatological record is not built upon hourly observations, percentiles are not directly calculated by binning the observations by numbers of occurrence. Since the upper-air and ocean data are compiled from twice-daily balloon launches (upper air), irregular aircraft and satellite measurements, and irregular ship observations (ocean), the historical records are in the form of mean and standard deviation data only. The ExpERT percentiles for the upper-air and ocean regions are projected from the mean and standard deviations, assuming either a normal or gamma distribution. The upper-air data in ExpERT are provided at every 1,000 ft (305 m) from the surface to 10,000 ft (3,048 m), every 2,000 ft from 10 to 20 kft, every 5,000 ft from 20 to 50 kft, and every 10 kft from 50 to 80 kft (Ref. 5). The ExpERT regions and sites as incorporated into HELEEOS are shown in Fig. 1.

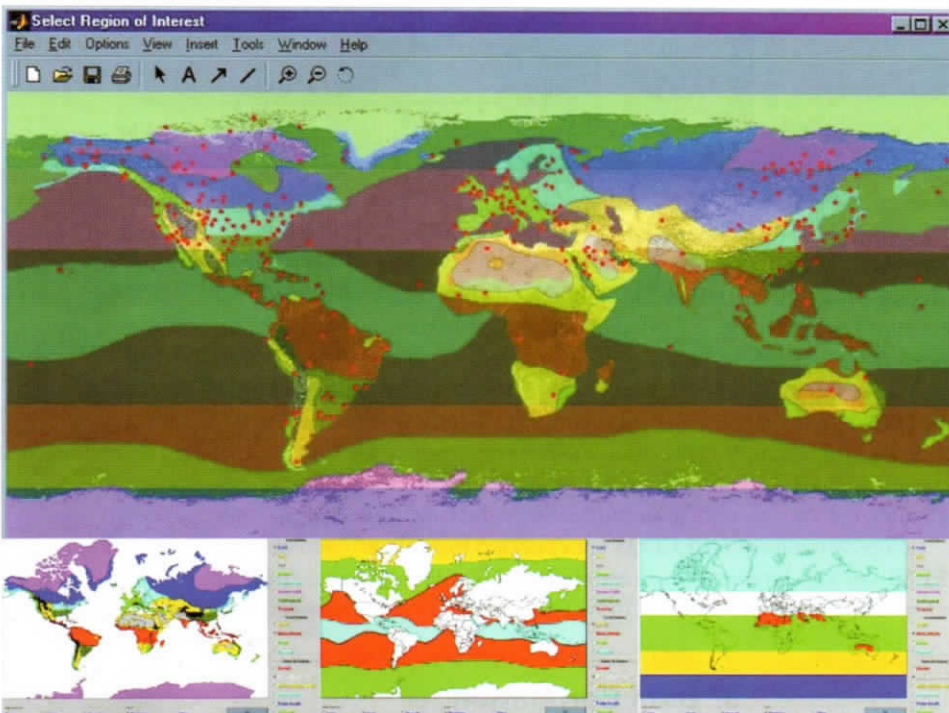


Fig. 1. Top panel: ExpERT-based HELEEOS surface sites plus eight land regions and four ocean regions overlaid with the six upper-air regions. Bottom three panels, left to right: separately displayed ExpERT land, ocean, and upper-air regions.

In the GADS incorporated into HELEEOS, the atmospheric aerosol particles are described by 10 main aerosol components, which are representative for the atmosphere and characterized through their size distribution and their refractive index depending on the wavelength. These aerosol particles are based on components resulting from aerosol emission and formation and removal processes within the atmosphere, so that they exist as mixtures of different substances, both external and internal. Typical components include water-soluble, water-insoluble, soot, sea salt, and mineral. The sea-salt particles are defined in two classes and the mineral particles in four. The GADS allows the display of the global aerosol distribution of each defined aerosol component, including the vertical profile, on a $5^\circ \times 5^\circ$ latitude-longitude grid for winter and summer. This permits the determination of the radiative properties and mass concentration of the resulting externally mixed aerosols at each grid point on the globe.⁷

The primary source for the HELEEOS optical turbulence data is the Master Database for Optical Turbulence Research in Support of Airborne Laser.³ The optical turbulence database is chiefly derived from thermosonde measurement vertical profiles at several sites worldwide. Thermosondes are balloon-borne payloads that measure in situ the temperature structure constant (C_T^2) using fine-wire probes separated by a 1-m horizontal distance. The C_T^2 parameter is measured approximately every 7–8 m in the vertical. The altitude range of thermosonde measurements is from the surface to 30 km above sea level. Owing to solar heating effects on the fine-wire probes, thermosonde measurements of C_T^2 are usually made at night. The thermosonde also measures pressure (p), temperature (T), humidity, and horizontal wind velocity using an attached, modified rawinsonde package. Neglecting water vapor fluctuations, this allows calculation of the index of refraction structure constant C_n^2 :

$$C_n^2 = C_T^2 \left[79 \times 10^{-6} \frac{p}{T^2} \right]^2 \quad (\text{m}^{-2/3}), \quad (1)$$

where the pressure has units of hPa and temperature is in K (Ref. 8).

The DEEST is an optical turbulence decision aid used to simulate directed energy weapon scenarios. Currently, DEEST uses the Air Force Weather Agency (AFWA) MM5 15-km-resolution forecast data. DEEST represents atmospheric optical turbulence with the refractive index structure parameter C_n^2 . To calculate atmospheric turbulence, DEEST combines various C_n^2 models: the CLEAR1 model is used in the upper atmosphere above the MM5 model ceiling, the Dewan model is used in the free atmosphere, and three different models are used in the boundary layer and surface layer. DEEST derives various optical turbulence quantities from C_n^2 ; for example, spherical-wave Rytov variance, isoplanatic angle, and Greenwood frequency. DEEST computations employ ray tracing within an atmospheric volume to calculate the various optical turbulence integrals and to determine opaque cloud obscuration.¹ Future versions of HELEEOS are expected to allow users to obtain C_n^2 values via either DEEST-derived forecasts or probabilistic climatological values from the Master Database for Optical Turbulence analysis done for HELEEOS and described in Sec. 4.

3. Data Correlation

The HELEEOS model incorporates and simulates numerous different probabilistic, and independently compiled, atmospheric variables. Since the model concentrates on uncertainty in the form of a user-defined “probability” or “percentile,” the realistic correlation of

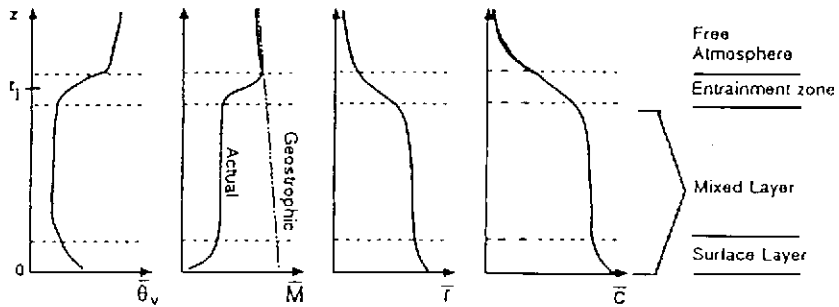


Fig. 2. Typical daytime vertical profiles of mean virtual potential temperature θ_v , wind speed M (where $M^2 = u^2 + v^2$), water vapor mixing ratio r , and pollutant concentration c . (Adapted from Fig. 1.9 of Stull.¹⁰)

the different independent variables at the specified level of uncertainty is paramount. This section addresses this correlation issue by outlining the percentiles utilized in the model, the method of choosing the “percentile of interest,” and how the determination of atmospheric values varies by altitude.

The ExPERT database enables HELEEOS to provide environmental probability density function (PDF) information in the form of nine different percentiles: 1, 5, 10, 20, 50, 80, 90, 95, and 99 percentile for summer and winter seasons. It provides this information for all land, ocean, and upper-air regions and the individual surface land sites. However, while the individual land sites each has a correlated temperature and relative humidity database, the upper-air and ocean data do not. Consequently, the individual surface site PDFs can be more meaningfully and realistically correlated than the PDFs aloft or for the ocean areas.

Given HELEEOS’s focus on lower-tropospheric engagements and the greater degree of correlation available from the surface land data, an assumption is made that the atmospheric boundary layer can be characterized by surface parameters. Assuming that the boundary layer is “well-mixed” and is therefore nearly homogeneous in its potential temperature (the temperature a parcel or layer would have if brought adiabatically to a pressure of 1,000 hPa), moisture, pollutant/aerosol, and wind-speed characteristics is consistent with Stull¹⁰ and many others conducting boundary-layer research. The homogeneity of an idealized boundary layer is illustrated in Fig. 2. Stull and others also indicate that the typical, fair weather, afternoon boundary layer extends up to about 1,500 m. Thus, the boundary layer is set to the lowest 1,500 m (~5,000 ft) in HELEEOS and is characterized by surface site values. There are inherent weaknesses associated with these assumptions—some of which are addressed in the conclusions—but for the early versions of HELEEOS they do not override the strength of greater data correlation within a “fair weather” (clear-line-of-sight) boundary layer.

As noted in the preceding section, ExPERT gives HELEEOS the ability to correlate the temperature and relative humidity PDFs for the individual sites, and therefore the boundary layer above those sites. Relative humidity is critically important in the growth and scattering effects of aerosols (described in the next section) and, when properly coupled with temperature, can yield correlated values of all other moisture parameters (i.e., mixing ratio, specific humidity, absolute humidity, and dew point). Thus, HELEEOS uses relative humidity as the key parameter in determining how the user-defined “percentile of interest” (or probability or uncertainty of interest) is converted into specific environmental values for HEL propagation calculations.

not a parameter in the ExPERT upper-air database; it must be derived from temperature and dew point. Since the temperature and dew point data are generally normally distributed in all regions, seasons, and altitudes,⁵ the 50 percentile data can be considered “correlated.” Thus, 50 percentile values of temperature and dew point are used to derive RH for aerosol size distribution, scattering, and absorption at altitudes above the boundary layer. The dry number density of aerosols above the boundary layer is varied exponentially with height as done in Hess et al.⁶:

$$N(h) = N(0)e^{-h/Z}, \quad (2)$$

where $N(0)$ is the boundary-layer aerosol number density, h the altitude above ground in kilometers, and $Z = 8$ km is the scale height of the atmosphere. For above-boundary-layer molecular absorption calculations, the user-defined percentile of interest determines a dew point percentile that gives a dew point temperature that yields the moisture content needed for water vapor absorption. For C_n^2 values above the boundary layer, the user-defined percentile is used to get a temperature that is then empirically related to a C_n^2 value.

4. Beam Spread and Attenuation Causes: Calculations and Discussion

The primary causes of HEL diffraction-limited beam spread and attenuation in a non-cloudy atmosphere are aerosol scattering and absorption, molecular absorption, and optical turbulence. For engagements in the lower troposphere, all of these effects play a significant role; however, water vapor (molecular) absorption is minimized in engagements with high-energy solid-state lasers (SSLs) tuned to operate in fully “clean-window” bands. This section details the calculations and manipulations necessary to allow HELEEOS to fully incorporate the above effects in a correlated, physically meaningful manner. Brief analyses of some of the preliminary results are also presented.

HELEEOS calculates an aerosol size distribution for each user-specified scenario, location, altitude, season, and relative humidity. For aerosol scattering and absorption calculations, Mie scattering is assumed. The dimensionless Mie extinction, scattering, and absorption coefficients are first calculated assuming a dry environment and then allowed to vary with increasing RH conditions.

The HELEEOS aerosol algorithm calculates dimensionless extinction, scattering, and absorption efficiencies with the Wiscombe¹¹ Mie scattering module. Wavelength-specific complex indices of refraction for the 10 GADS aerosol species are interpolated from either Table 4.3 in d’Almeida et al.⁴ or using tables derived with the Optical Properties of Aerosols and Clouds (OPAC) software package.⁶ The normalized radius-specific particle number density per unit volume [$dN/d(\log r)$] is derived as shown in d’Almeida et al.⁴ for the log-normal distribution:

$$\frac{dN(r)}{d(\log r)} = \frac{N}{(2\pi)^{1/2} \log(\sigma)} \exp\left[-\frac{(\log r - \log r_M)^2}{2(\log \sigma)^2}\right], \quad (3)$$

where N is the total particle number density per unit volume and is normalized to 1. The r_M value is the modal (or median) radius, and σ is the standard deviation for the aerosol species. HELEEOS takes these values from either d’Almeida et al.⁴ or Hess et al.⁶ As done in d’Almeida et al., the wavelength-specific normalized extinction, scattering, and

absorption coefficients [$\sigma_{e,s,a}(\lambda)$] are obtained by integrating over the range of radii using

$$\begin{aligned}\sigma_{e,s,a}(\lambda) &= \int_{r_1}^{r_2} Q_{e,s,a}(m, \lambda, r) \pi r^2 \frac{dN(r)}{r \ln 10 d(\log r)} dr \\ &\approx \sum_{i=r_{\min}}^{r_{\max}} Q_{e,s,a}(m, \lambda, r_i) \pi r_i^2 \frac{dN_i}{r_i \ln 10 d(\log r_i)} \Delta r_i.\end{aligned}\quad (4)$$

For moist aerosol calculations one must consider that humidity causes aerosol particle growth, even at RH values far below saturation. d'Almeida et al. handle this by allowing the modal radius and the refractive index for each aerosol species to vary with RH. The standard deviation and the particle number density of the log-normal distribution for each species are not varied with RH. HELEEOS calculates the humidity-altered radius value, $r(a_w)$, by obtaining the particle number density from Eq. (3) (using the dry r_M and σ) and then solving Eq. (3) for $r(a_w)$ using the humidity-specific r_M and holding the particle number density [$dN/d(\log r)$] constant. This is described by the following:

$$\log r(a_w) = \pm \left[-\ln \left(\text{ND} \sqrt{2\pi} \log \sigma \right) \cdot 2(\log \sigma)^2 \right]^{1/2} + \log r_M, \quad (5)$$

where $\text{ND} = dN/d(\log r_o)$, σ = the standard deviation from d'Almeida et al. or Hess et al., and r_M = the modal radius for the given RH. [Note that the first term on the right-hand side of Eq. (4) is negative when ND is calculated using a dry particle radius, $r_o < 1 \mu\text{m}$, and positive when $r_o \geq 1 \mu\text{m}$.] HELEEOS considers aerosols "dry" if $\text{RH} < 50\%$. For $\text{RH} \geq 50\%$, modal radii are interpolated from the values given in Table 6.2 of d'Almeida et al.

Moist growth of aerosol particles changes not only their size, but also their index of refraction. HELEEOS again follows d'Almeida et al. and derives the humidity-altered index of refraction from

$$n = n_w + (n_o - n_w) \left[\frac{r_o}{r(a_w)} \right]^3, \quad (6)$$

where $n = m_r + i m_i$, n_w is the refractive index for liquid water, n_o is the refractive index for the dry particles, r_o is the radius of the dry particles, and $r(a_w)$ is the radius of the particle at the given RH, obtained with Eq. (5). With the humidity-altered radius value and index of refraction, HELEEOS reinvokes the Wiscombe module to get RH-modified Mie efficiencies and then uses Eq. (3) for RH-modified normalized radius-specific particle number density per unit volume [$dN/d(\log r)$].

While Eqs. (3)–(6) and knowledge of the RH provide a means for HELEEOS to assess aerosol scattering and absorption, molecular extinction requires knowledge of water vapor density (absolute humidity) and carbon dioxide (CO_2). For HEL scenarios involving wavelengths greater than $1 \mu\text{m}$, molecular extinction is virtually all due to molecular absorption effects as scattering effects become almost nonexistent. For the chemical oxygen-iodine laser (COIL) and other HEL lower atmosphere applications at or near water vapor absorption lines, the molecular absorption is predominately caused by gaseous water, with CO_2 as a much smaller secondary contributor. For HELs at non-water-absorbing wavelengths, CO_2 is the primary molecular absorber. HELEEOS derives the CO_2 -number-density-based pressure and an assumption that atmospheric composition is homogenous throughout all modeled engagement altitudes. In the boundary layer, the model obtains absolute humidity from RH and correlated temperature and pressure. Above the boundary layer, HELEEOS uses temperature, dew point temperature, and pressure to obtain the absolute humidity.

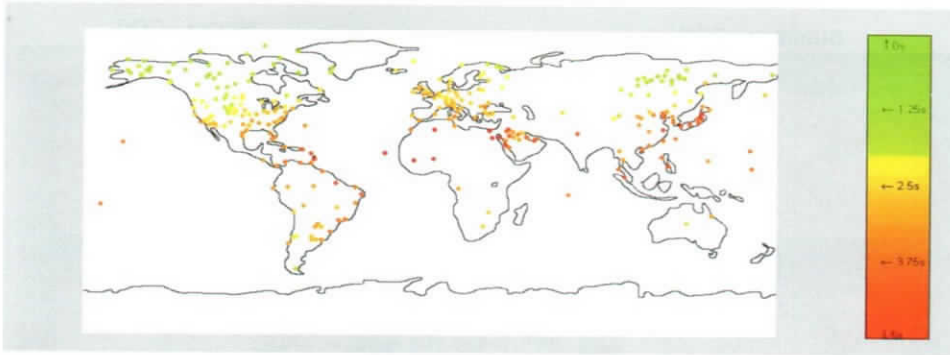


Fig. 4. Worldwide analysis (with winter 50 percentile water vapor and aerosol data) of dwell time required to achieve a user-specified P_k for user-specified RH conditions (percentile), season, weight-constrained laser type, and engagement geometry. Case shown is for a COIL, wavelength $\sim 1.315 \mu\text{m}$. Both northern and southern hemispheres are shown in summer conditions.

Because HELEEOS performs simulations at only a few specific wavelengths (e.g., 1.06 and $1.315 \mu\text{m}$), the atmospheric transmission algorithms necessary to obtain molecular absorption from vapor density and CO_2 number concentration are fully encoded within the model and are described in Bartell et al.²

Incorporation of aerosol scattering and molecular absorption into HELEEOS HEL engagement scenarios significantly affects simulated dwell times. This is illustrated in Fig. 4, where regions with relatively low summer RH and absolute humidity are generally characterized with low (“green”) dwell times. The aerosol scattering effect is generally at least an order of magnitude larger than the aerosol absorption effect. Thus, areas with orange and red sites in Fig. 4 exhibit longer required dwell times due to high absolute humidity (case shown is for the COIL), high relative humidity, high aerosol content, or a combination of two or more of these factors. Figure 5 displays both COIL ($1.315 \mu\text{m}$) and SSL ($1.06 \mu\text{m}$) worldwide trials for both summer and winter cases, at three increasing RH percentiles. The COIL’s sensitivity to absolute humidity is apparent in the difference in winter and summer dwell times at all the RH percentiles. Notable, however, is that the dwell times increase with increasing RH percentile for both the COIL and SSL, in both winter and summer. This strongly suggests that the more dominant atmospheric effect is aerosol scattering, even when the COIL sensitivity to water vapor absorption is considered.

There are significant operational implications of the effects of aerosol scattering, and the modulating effects of RH on the scattering, on lower troposphere HEL engagements. Because the absolute range of RH across the three percentiles shown in Fig. 5 is frequently experienced at every site on a diurnal basis, a HEL engagement may be subjected to a two- to threefold increase or decrease in dwell time simply by changing the time of day of the scenario. An example of this is shown in Fig. 6, a depiction of a fair-weather day at Wright–Patterson Air Force Base, Ohio. The conditions shown in Fig. 6, where the temperature cycles with solar heating and moisture (measured in dew point temperature) remains fairly constant, are typical of any fair-weather day at any location in the world. This cycle of temperature and moisture causes a fluctuation of RH from 100% to $\sim 25\%$ back again to 100% over less than 18 h. During periods of reduced scattering (e.g., afternoon times), HELEEOS predicts the possibility of more thermal blooming due to absorption. One could

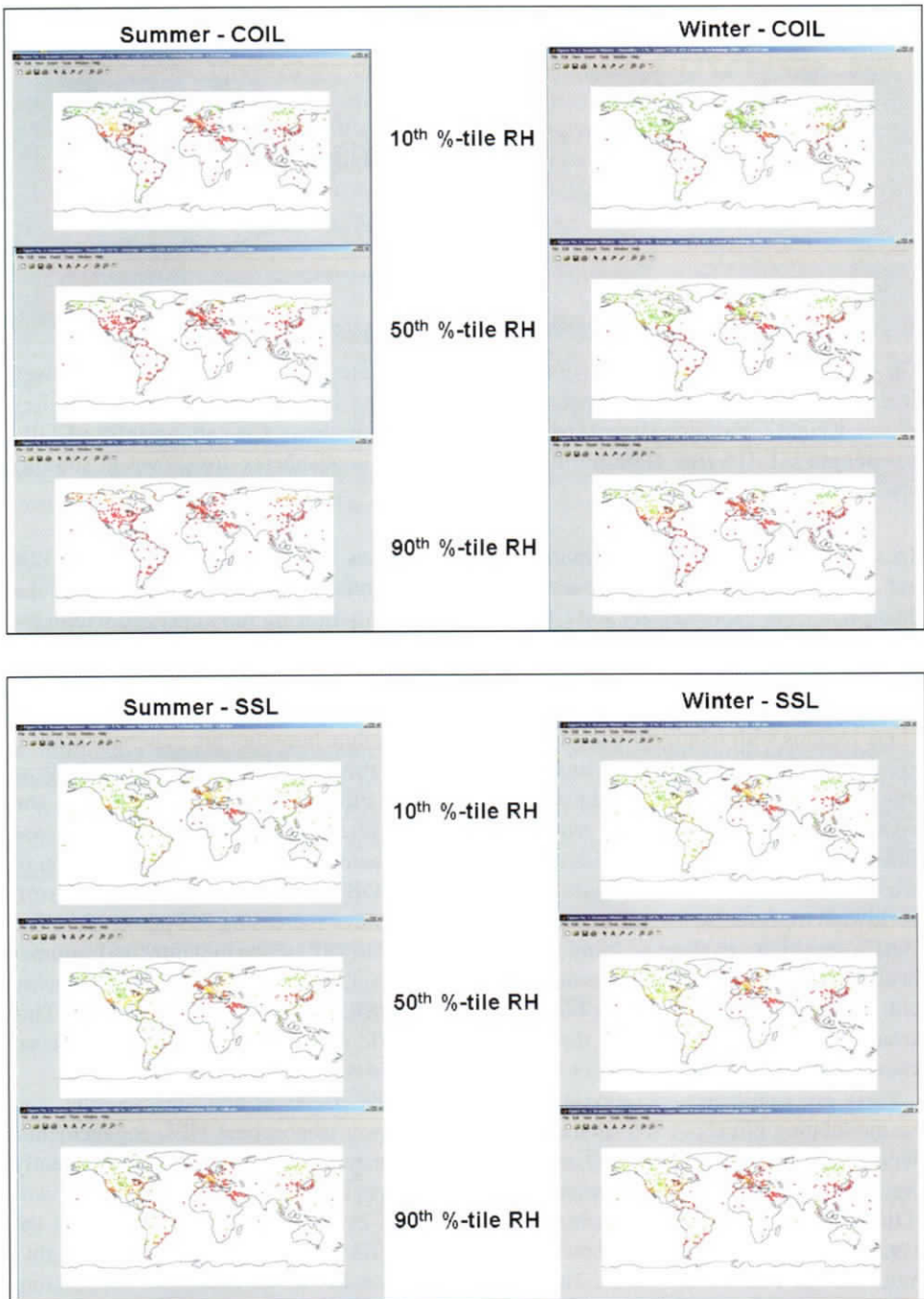


Fig. 5. Worldwide P_k trials for the COIL (top panels) and the solid-state laser (SSL; bottom panels) at the three different RH percentiles displayed, in summer and winter. The individual sites are color coded according to required dwell time in the same manner as in Fig. 4. Charts are not directly comparable to Fig. 4 due to differences in user-specified P_k and engagement geometry.

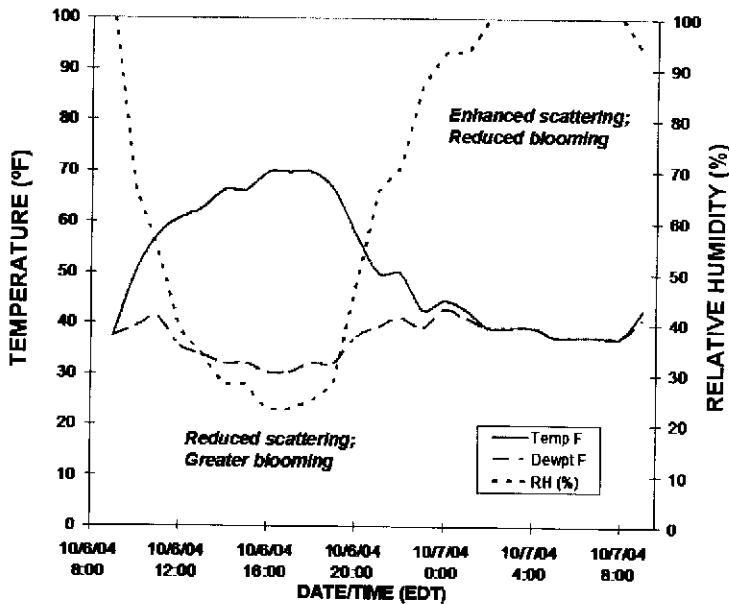


Fig. 6. Chart depicting temperature, dew point, and RH variations at Wright-Patterson Air Force Base, Ohio, on Oct. 6–7, 2004. Periods with lower (higher) RH are noted as times with reduced (enhanced) aerosol scattering and thus greater (reduced) thermal blooming effects.

conversely expect reduced thermal blooming effects during periods of higher scattering (e.g., nighttime, early morning) due to high RH.

HELEEOS has aspects of the DEEST environmental data tool built into it mainly so that it can obtain optical turbulence data for simulation. The DEEST-derived C_n^2 profiles are an excellent source of forecast data; however, they are for the most part deterministic in nature. To acquire a probabilistic optical turbulence database for use in HELEEOS, the thermosonde data noted in Sec. 2 from several representative sites were analyzed to describe C_n^2 distributions within the boundary layer and at various altitudes above it. This analysis found that regardless of whether C_n^2 was being empirically related to RH or temperature and altitude, the distributions could be well-fitted to a lognormal curve. Thus, HELEEOS uses climatologically representative lognormal distribution curves to probabilistically characterize optical turbulence. The lognormal distribution data are stored for the representative boundary layers and above-boundary-layer-altitude bins with five unique coefficients of the following equation:

$$x = \left[\exp\left(\frac{\pm 1}{\ln(2)} \cdot \left\{ \ln(2) \cdot \ln\left[\frac{(y-a)}{b}\right]\right\}^{0.5} \cdot \ln(e)\right) \cdot d \cdot (e-1) + c \cdot e^2 - c \right] / (e^2 - 1). \quad (7)$$

Figure 7 provides examples of three boundary-layer C_n^2 distributions and three different temperature/altitude bin distributions above the boundary layer. The five unique coefficient values are included for one of the distributions.

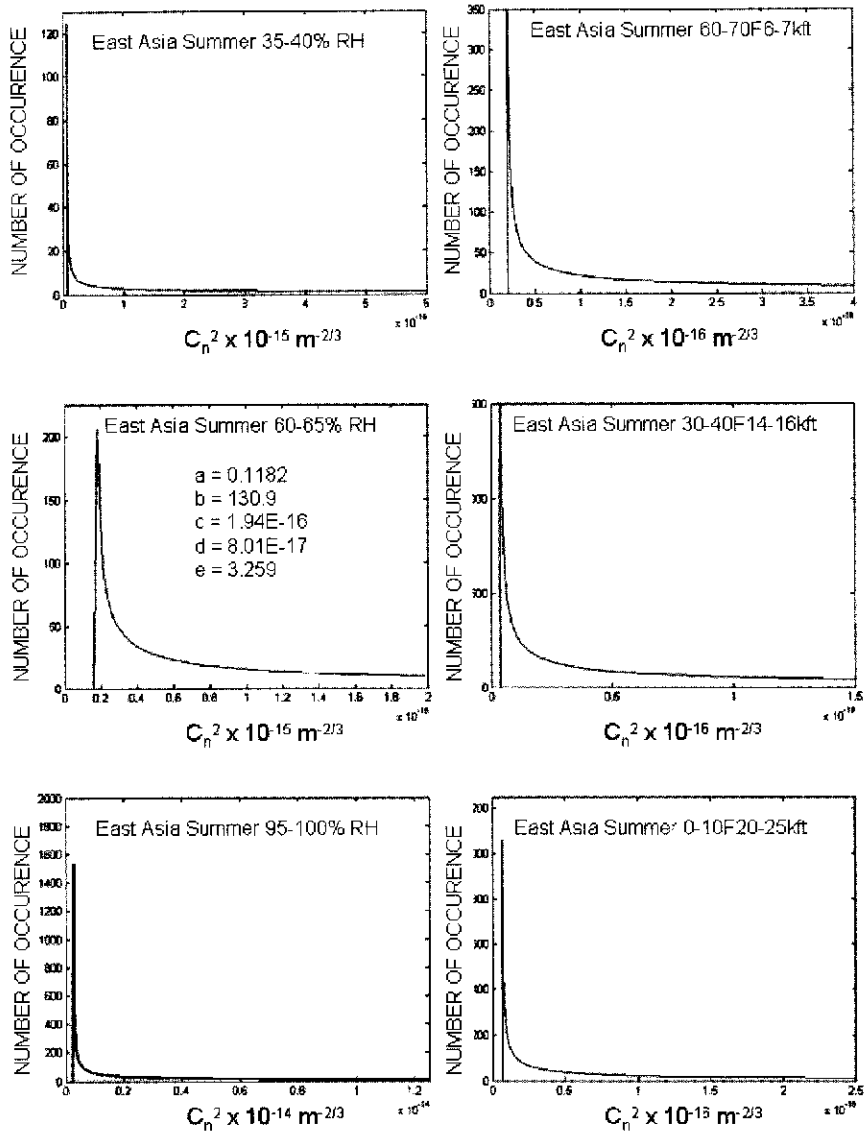


Fig. 7. Example C_n^2 distributions for three boundary layer (left panels) cases binned by associated relative humidity. Right panels show cases above the boundary layer where C_n^2 is binned by associated temperature and altitude.

5. Summary/Conclusions

The HELEEOS atmospheric effects package demonstrates several significant improvements in the realm of HEL engagement simulation. Foremost, it provides HELEEOS with a self-contained, correlated, and probabilistic atmospheric database. This database permits the model a great degree of flexibility in modeling HEL engagements, anywhere, anytime in the world—and provides realistic degradation effects on propagation. This, in turn, enhances

HELEEOS's ability to characterize uncertainty and risk in the bottom line of probability of kill.

The research that produced the atmospheric effects package is still on-going. However, the preliminary conclusion that aerosol scattering effects outweigh all other environmental effects—even in the COIL case—for lower-troposphere HEL engagements is significant and should be noted at this juncture prior to completion of research. Furthermore, the operational implications noted in this research (see Fig. 6) of the effects of very common diurnal RH fluctuations on aerosol scattering warrant attention and additional study.

This research has also highlighted some areas for future HELEEOS add-ons and/or improvements. As pointed out in Sec. 3, HELEEOS could be enhanced with diurnal atmospheric data. This would allow not only for simulating the RH fluctuations addressed in the preceding paragraph, but also for boundary-layer height variations based on time of day. Some areas for improvement are being developed as of this writing. Those include the Air Force Combat Climatology Center's effort to process up to thousands more ExPERT sites, and AFIT's in-house project to allow HELEEOS users to access, display, and export atmospheric data independent of a HEL engagement simulation. Additional improvement areas are under consideration as well, such as allowing user selection of any wavelength between 0.4 and 14 μm , with a set of up to 20 select wavelengths supported via lookup table for runtime advantage; providing representations of water cloud, fog, and light-rain effects; support for user-specified surface visibility; enhancements to atmospheric boundary-layer calculations, specifically temperature and dew point lapse rates within the boundary layer that would produce more realistic RH-based aerosol effects; incorporation of the latest HITRAN line strength data for molecular absorption calculations of the top 13 molecular absorbers, rather than only water vapor and carbon dioxide; integration of probabilistic wind speed data for all ExPERT sites; and inclusion of single-scattering phase function information along the beam axis.

References

- ¹Adair, S.C., G.T. Fairley, and G.Y. Jumper, "The Directed Energy Environmental Simulation Tool: Features and Philosophy," Presented at the Battlespace Atmospheric and Cloud Impacts on Military Operations (BACIMO) 2003, NRL, Monterey, CA (2003).
- ²Bartell, R.J., G.P. Perram, S.T. Fiorino, S.N. Long, M.A. Marciniak, M.J. Houle, C.A. Rice, Z.P. Manning, S.T. Haschke, D.W. Bunch, M.J. Krizo, and L.E. Gravley, *J. Directed Energy*, in preparation.
- ³Bussey A.J., J.R. Roadcap, R.R. Beland, and G.Y. Jumper, "Master Data Base for Optical Turbulence Research in Support of Airborne Laser," Air Force Research Laboratory Technical Report, AFRL-VS-TR-2000-1545 (2000).
- ⁴d'Almeida, G.A., P. Koepke, and E.P. Shettle, *Atmospheric Aerosols: Global Climatology and Radiative Characteristics*, A. Deepak Publishing (1991).
- ⁵Fiorino, S.T., and D.L. Parks, "Regional and Worldwide Atmospheric Profiles for MERIT," Institute of Environmental Sciences 1995 Proceedings, 41st Annual Meeting (1995).
- ⁶Hess, M., P. Koepke, and I. Schult, *Bull. Am. Met. Soc.*, **79**, 831 (1998).
- ⁷Koepke, P., M. Hess, I. Schult, and E.P. Shettle, "Global Aerosol Data Set," MPI Meteorologic Hamburg Report No. 243 (1997).
- ⁸Roadcap, J.R., P.J. McNicholl, and R.R. Beland, "Analysis of Thermosonde Data for High Energy Laser Tactical Applications." Presented at the Battlespace Atmospheric and Cloud Impacts on Military Operations (BACIMO) 2003, NRL, Monterey, CA (2003).
- ⁹Squires, M.F., B.A. Bietler, S.T. Fiorino, D.L. Parks, F.W. Youkhana, and H.D. Smith, "A Method for Creating Regional and Worldwide Datasets of Extreme and Average Values," Institute of Environmental Sciences 1995 Proceedings, 41st Annual Meeting (1995).
- ¹⁰Stull, R.B., *An Introduction to Boundary Layer Meteorology*. Kluwer Academic Press (1989).
- ¹¹Wiscombe, W.J., *Appl. Opt.* **19**(9), 1505 (1980).

The Authors

Mr. R. J. Bartell received his B.S. degree in Physics from the U.S. Air Force Academy as a distinguished graduate in 1979. He received his M.S. degree from the Optical Sciences Center, University of Arizona, in 1987. He is currently a Research Physicist with the Engineering Physics Department of the Air Force Institute of Technology, where he leads the development of the High Energy Laser End-to-End Operational Simulation (HELEEOS) model.

Mr. Dustin Bunch worked as an undergraduate research assistant at AFIT and contributed to the research for this project. He received a B.S.E.E. degree from Cedarville University in 2005.

Lt. Col. Steven Fiorino is an Assistant Professor of Atmospheric Physics at the Air Force Institute of Technology (AFIT). He has B.S. degrees in Geography and Meteorology from Ohio State (1987) and Florida State (1989) universities. He additionally holds an M.S. in Atmospheric Dynamics from Ohio State (1993) and a Ph.D. in Physical Meteorology from Florida State (2002). His research interests include microwave remote sensing, development of weather signal processing algorithms, and atmospheric effects on military systems such as high-energy lasers and weapons of mass destruction.

Ms. Liesebet Gravley graduated from Wittenberg University in 2004 with a Bachelor of Arts in Physics and German. During the summer of 2005, she was hired as a Directed Energy Professional Society (DEPS) intern, where she did research on characterizing optical turbulence. Currently, she is a graduate student at the Air Force Institute of Technology and studying applied physics.

Mr. Matthew Krizo is a student research assistant who has performed much of the programming of HELEEOS since 2004. He received his B.S.E.E. from Cedarville University in 2005 and is currently working on a M.S. at the University of Dayton.

Mr. Zachary Manning worked as an undergraduate research assistant at AFIT and contributed to the research for this project.

Dr. Glen Perram received his B.S. degree in Applied Physics from Cornell University in 1980 and his M.S. and Ph.D. degrees in Physics from the Air Force Institute of Technology in 1981 and 1986, respectively. He is currently Professor of Physics at AFIT, having served as a member of the faculty since 1989. Professor Perram's research interests include chemical lasers, remote sensing, optical diagnostics, and laser weapons systems modeling.

Mr. Christopher Rice completed his undergraduate studies at Cedarville University in Cedarville, Ohio, earning a B.S.E.E. Currently, Mr. Rice is working in the field of modeling and simulation as a contractor for Booz Allen Hamilton at Wright-Patterson AFB and is completing his M.S.E.E. at AFIT.